Accepted Manuscript

Sol-gel deposition of hydroxyapatite coatings on porous titanium for biomedical applications

C. Domínguez-Trujillo, E. Peón, E. Chicardi, H. Pérez, J.A. Rodríguez-Ortiz, J.J. Pavón, J. García-Couce, J.C. Galván, F. García-Moreno, Y. Torres

PII: S0257-8972(17)31120-9
DOI: doi:10.1016/j.surfcoat.2017.10.079
Reference: SCT 22844

To appear in: *Surface & Coatings Technology*

Received date: 17 August 2017
Revised date: 2 October 2017
Accepted date: 31 October 2017

Please cite this article as: C. Domínguez-Trujillo, E. Peón, E. Chicardi, H. Pérez, J.A. Rodríguez-Ortiz, J.J. Pavón, J. García-Couce, J.C. Galván, F. García-Moreno, Y. Torres , Sol-gel deposition of hydroxyapatite coatings on porous titanium for biomedical applications. The address for the corresponding author was captured as affiliation for all authors. Please check if appropriate. Sct(2017), doi:10.1016/j.surfcoat.2017.10.079

This is a PDF file of an unedited manuscript that has been accepted for publication. As a service to our customers we are providing this early version of the manuscript. The manuscript will undergo copyediting, typesetting, and review of the resulting proof before it is published in its final form. Please note that during the production process errors may be discovered which could affect the content, and all legal disclaimers that apply to the journal pertain.

ACCEPTED MANUSCRIPT

SOL-GEL DEPOSITION OF HYDROXYAPATITE COATINGS ON POROUS TITANIUM FOR BIOMEDICAL APPLICATIONS

C. Domínguez-Trujillo[1], E. Peón[2], E. Chicardi[1*], H. Pérez[2], J.A. Rodríguez-Ortiz[1], J.J. Pavón[3], J. García-Couce[2], J.C. Galván[4], F. García-Moreno[5] and Y. Torres[1]

[1] *Department of Engineering and Materials Science and Transportation, Polytechnic School of Seville (EPS), University of Seville (US), Virgen de Africa 7, 41011 Seville, Spain.*

[2] *Biomaterials Center (BIOMAT), University of La Habana (UH), La Habana 10600, Cuba.*

[3] *Group of Advanced Biomaterials and Regenerative Medicine, BAMR, Bioengineering Program, University of Antioquia, Calle 67 No. 53-108, Medellín, Colombia.*

[4] *National Centre for Metallurgical Research, CENIM-CSIC, Gregorio del Amo Avenue 8, 28040 Madrid, Spain.*

[5] *Helmholtz Zentrum Berlin, Institute of Applied Materials, Hahn-Meitner-Platz 1, 14109 Berlin, Germany.*

ACCEPTED MANUSCRIPT

ACCEPTED MANUSCRIPT

ABSTRACT

The stress shielding and the poor osseointegration in titanium implants are still problems to be resolved. In this context, this work proposes a balanced solution. Titanium samples were fabricated, with a porosity of 100-200 μm of pore size employing space-holder technique (50 vol. % NH_4HCO_3, 800 MPa at 1250 ºC during 2h under high vacuum conditions), obtaining a good equilibrium between stiffness and mechanical resistance. The porous titanium substrates were coated with hydroxyapatite, obtained by sol-gel technique: immersion, dried at 80ºC and heat treatment at 450ºC during 5h under vacuum conditions. Phases, surface morphology and interfacial microstructure of the transverse section were analyzed by Micro-Computed Tomography, SEM and confocal laser, as well as the infiltration capability of the coating into the metallic substrate pores. The FTIR and XRD showed the crystallinity of the phases and the chemical composition homogeneity of the coating. The size and interconnected pores obtained allow the infiltration of hydroxyapatite (HA), possible bone ingrowth and osseointegration. The scratch resistance of the coating corroborated a good adherence to the porous metallic substrate. The coated titanium samples have a biomechanical and biofunctional equilibrium, as well as a potential use in biomedical applications (partial substitution of bone tissue).

Keywords: Space-holder; hydroxyapatite; porous titanium; sol-gel: stress shielding; osseointegration,

* Corresponding author: echicardi@us.es

ACCEPTED MANUSCRIPT

1. INTRODUCTION

Bone tissues are affected by the aging of people and diseases. Commercial pure Titanium (c.p. Ti) and the alloy Ti_6Al_4V are well known biomaterials and clinically accepted thanks to their good mechanical properties and corrosion resistance in physiological fluids [1, 2]. Nevertheless, they still exhibit some problems which have to be resolved: the biomechanical (stress-shielding phenomenon) [3] and the biofunctional (poor osseointegration) [4]. The stiffness discrepancy between the implant and the bone tissue can be addressed by making porous materials. In addition, the generated pores could improve bone ingrowth towards the interior of the implant (with an optimal pore size) [2, 5] and the enhancement of the osseointegration thanks to the roughness [6] within the pore [7]. On the other hand, the surface of the implant must be modified to improve the osseointegration capacity and avoid the micro movements at the implant-bone interface [2]. The use of bioactive HA coatings promotes the bone formation, the adhesion and the fixation of the metallic substrates [2, 8]. In the literature, different deposition techniques are reported not only for bioactive HA, but also for other coatings: sol-gel, electrochemical, electrophoretic, micro-arc, plasma spraying, sputter, hot isostatic pressing, pulsed laser, magnetron sputtering, chemical vapor deposition (CVD), biomimetic, among others [9-13]. The sol-gel technique allows a thin HA film on porous Ti substrates to be obtained [14-16], achieving a good chemical homogeneity. Within this framework, this work proposes the production of porous titanium substrates coated with HA as a potential solution for obtaining the desired biomechanical and biofunctional balance.

ACCEPTED MANUSCRIPT

2. MATERIALS AND EXPERIMENTAL PROCEDURE

Porous titanium substrates (grade IV) were fabricated by space-holder technique [17, 18], employing ammonium hydrogen carbonate, NH_4HCO_3 as space-holder (50 vol. % and a particle size range of 100-200 μm). The content employed was chosen according to the previous works of the authors [19]. The powders were mixed by using a Turbula® T2C for 40 mins to achieve a good homogenization. The blend was pressed to 800 MPa using an Instron 5505 universal testing machine. The space holder was then removed in a furnace in two steps of 12h each (at 60°C and 110°C, both under low vacuum conditions of ~10-2 mbar). Finally, the green compacts were sintered in a Carbolyte® STF 15/75/450 ceramic furnace, with a horizontal tube at 1250°C for 2h using high vacuum (~10-5 mbar). The protocol used for the HA coating is a variant of one procedure shown in the literature [20-23]. The precursor was triethyl phosphite, hydrolyzed during 24h with distilled water under vigorous stirring. The required stoichiometric amount of calcium nitrate (Aldrich) solution was then added to the hydrolyzed solution. The mixture was additionally stirred and allowed to rest for 24h. The metallic substrate was then coated by dip-coating and drying at 80°C overnight. The coating adherence was improved by submitting the substrates to a thermal treatment at 450 ºC for 5h under vacuum conditions.

The interconnected (P_i) and total porosity (P_T) of porous titanium substrate were obtained by Archimedes' method (ASTM C373-14). Image analysis (IA) was employed to determine the equivalent diameter of the pores, using a Nikon Epiphot optical microscope coupled with a Jenoptik Progres C3 camera and Image-Pro Plus 6.2 analysis software [24].

ACCEPTED MANUSCRIPT

Also, X-ray computed tomography (M-CT) was used to compare the porosity values and the equivalent porous diameter obtained by Archimedes' and Image Analysis, respectively. For this purpose, a micro focus X-ray source L8121–01, operating at 100 kV, 100 mA, 5 mm of spot size and a flat panel detector C7943 (120 mm × 120 mm, 2400 2240 × 2400 2368 pixel), both from Hamamatsu Photonics K.K. (Japan), were employed. Through this methodology, a qualitative and quantitative study was carried out of the interior structure of the porous Ti sample used as substrate before HA deposition. A maximum spatial resolution of 6.4 microns per pixel was reached at 7.8x magnification. Concretely, a porous Ti disc substrate was studied and a 3D image for this specimen was obtained by the acquisitions of a high number of X-ray projections during 360º sample rotation in 1000 steps. The reconstructed complete volume of the porous Ti disc was subjected to image analysis, including a series of filtering, separation and segmentation steps. After reconstruction, the commercial software VGStudioMax 1.2.1 (Volume Graphics, Heidelberg, Germany) was used to extract 2D and 3D sections of the foam. Also, the software MAVI 1.3.1 (Fraunhofer ITWM, Kaiserslautern, Germany) was used for volume image analysis of the tomographic data sets [25].

The mechanical behavior was measured by ultrasound technique (dynamic Young's modulus employing a KRAUTKRAMER USM 35 equipment) [26, 27] and uniaxial compression testing (stiffness and yield strength, performed by Instron 5505 universal testing machine) [28, 29]. Confocal microscopy (MC, Sensofar S Neox) and scanning electron microscopy (SEM, Tescan Vega TS 5130SB) were employed to analyze the topography roughness of the coating surface [30], and associated energy dispersive spectroscopy (EDS-Oxford Inca) was used to determine the elemental composition of the HA coating. Furthermore, Fourier Transform Infrared Spectroscopy

ACCEPTED MANUSCRIPT

(FTIR-ABB Bomem Inc., MB series) with a reflectance stage, recorded in the range of 400–4000 cm-1, and X-ray diffraction (XRD - D8, Focus, Brucker), performed with CuKα radiation (30 kV, 50 mA) were employed to characterize the HA coating. Finally, the scratch test was performed by a MICROTEST commercial device (MTR3/50-50/NI, Rockwell diamond tip with a diameter of 200 μm, applied load from 0 to 25 N, speed 0.5 mm/min and 5 mm of groove, according to ASTM C1624-05).

ACCEPTED MANUSCRIPT

ACCEPTED MANUSCRIPT

3. RESULTS AND DISCUSSION

The interconnected porosity value obtained (43%) was close to that of the total porosity (45%). The equivalent diameter by IA (161 μm) is in the size range of the chosen spacer particles (100-200 μm), as expected (Fig. 1a). Total pore fraction, mean size and the high degree of interconnectivity ensure the bone ingrowth and the infiltration of HA [31].

The dynamic Young's modulus (E_d = 20.8 GPa) and compression test behavior (E_c = 26.0 GPa and σ_y = 127 MPa) of porous titanium substrate ensure a reduction of the mismatch between the properties of cortical bone (20-25 GPa and 150-180 MPa) and the implant. The micro-hardness values after Vickers micro indentation of $HV_{0.3}$ and HV_1 were 401 and 167 respectively. In addition, the roughness within the pores (Fig. 1) improves the osseointegration, as cellular adhesion was demonstrated in previous works of the authors [19, 32].

A total volumetric porosity value of 49.8 %, and an equivalent porous diameter (D_{eq}) of 173 μm, were obtained by X-ray computed tomography (M-CT). Both characteristic parameters are in the range of the expected nominal values (50% volume fraction and Deq of spacer particle size between 100-200 μm). Thus, the spacer-holder technique was successfully employed to maintain the designed porosity parameters. These values were very close to those obtained by Archimedes' (45% of total volumetric porosity and 161μm of D_{eq}). Therefore, both techniques are valid to adequately determine both microstructural parameters.

Figure 2a shows the distribution of roughness volume percentage (relative roughness, forward), determined as described by Yin et al [33, 34], based on the relation of the pore volume to the eroded, smoothed volume of the same pore analyzed

ACCEPTED MANUSCRIPT

quantitatively from the tomographies in the reconstructed 3D image of the studied porous Ti disc substrate. Common values for the roughness volume percentage between 10-15 % can be observed. However, the dispersion detected in this Fig. 2a is much higher, finding particles with roughness volume percentage from 5 % to more than 60 %. This could be due to high porosity dispersion. The higher values could even be attributable to micropores, inherent to the sintering process.

In turn, Fig. 2b shows the corresponding roughness volume percentage with the equivalent diameter pore size. The relative volume roughness increases with decreasing equivalent diameter. Obviously, the smaller pores show a much larger surface roughness and, consequently, higher relative roughness. However, the exponential behavior suggests another effect, based on the more reactive sintering of samples with smaller pores, and thus, higher relative roughness.

Finally, it is important to note that the higher pore equivalent diameter, the larger is the scattering of the roughness volume percentage. This fact again suggests the more reactive sintering of smaller pores, giving a higher but narrow relative roughness.

Fig. 3 shows the morphology of the HA coating by SEM. The formation of polycrystalline aggregates of hydroxyapatite nanoparticles (HA nanocrystallites) was observed [35]. The coating presents homogenous morphology, with no presence of cracks and/or discontinuities. Apparently, the surface area shows potential nucleation sites for the precipitation of apatite in the presence of biologic fluids, due to its morphology, roughness and the existence of pores. This implies a greater bonding adherence between the bone and the implant [36].

By other hand, it was detected and quantified by EDX the three majority elements expected in HA, i.e., Ca (43 ± 3), P (11 ± 2) and O (46 ± 3), determined all of

ACCEPTED MANUSCRIPT

them in weight %. In addition, the absence of peaks in the EDXs corresponding to waste elements or to metallic substrates confirms the coating homogeneity and continuity.

By other hand, regarding the FTIR spectra (Fig. 4a), the reflections of $\nu_4PO_4^{3-}$, $\nu_1PO_4^{3-}$ and $\nu_3PO_4^{3-}$ show the polyhedrons of PO_4^{3-} reordering in the crystal structure, as a result of the HA transformation from an amorphous to a crystalline phase. Also, the XRD pattern is shown in Fig. 4b. A high crystallinity is achieved after heat treatment at 450ºC, being lower in the results reported in the literature at lower temperatures [7]. The peaks found are characteristic of the HA phase (according to the map library PCPDFWIN v. 2.4 # 09-0432 o JCPDS 9-432); calcium phosphate peaks are not detected. Again, it is observable that the HA coating changes form an amorphous to a crystalline state [37]. In addition, good HA infiltration into the pores and adhesion of the coating is very important in achieving the osseointegration.

Fig. 5 shows the surface topography by laser confocal microscopy. The roughness increases once the substrate is coated as a result of heterogeneity coating (thickness variation of HA layer, presence of a micro porous coating and small amounts of debris associated with chipping in some areas).

The penetration resistance during scratching of HA-coated titanium substrates is shown in Fig. 6. This behavior depends on applied load and coating-substrate system (coating adhesion grade, micro-hardness and micro-porosity of the coating, as well as the pore size and stiffness of the substrate).

ACCEPTED MANUSCRIPT

4. CONCLUSIONS

The feasibility of the fabrication of porous titanium substrates by the space-holder technique was validated. The sol-gel route in HA formation was verified, it being possible to obtain HA porous thin films on porous titanium substrates employing a new heat treatment at 450 ºC. The crystalline structure of HA was confirmed by XRD and FTIR. A good attachment between the HA coatings and Ti substrates was observed, thanks to mechanical interlocking and possible chemical bonding. The HA coatings imply the prevention of the release of metal ions (more resistance to corrosion) and the metal surface being made bioactive. The proposed coating-porous substrate system allows a biofunctional (formation and growth of bone tissue over the surface and within the pores) and biomechanical (porous substrate properties: E_d = 21 GPa and σ_y = 127 MPa, close to those of cortical bone) balance.

ACCEPTED MANUSCRIPT

ACCEPTED MANUSCRIPT

ACKNOWLEDGMENTS

This work was supported by the Junta de Andalucía-FEDER (Spain) through the Project Ref. P12-TEP-1401 and by the Spanish Ministry of Economy and Competitiveness under the Grant No. MAT2015-71284-P. The authors would also like to thank the Technician, J. Pinto, for assistance in the scratch tests.

ACCEPTED MANUSCRIPT

ACCEPTED MANUSCRIPT

REFERENCES.

[1] L. Kunčická, R. Kocich, T.C. Lowe, Advances in metals and alloys for joint replacement, Progress in Materials Science, 88 (2017) 232-280.
[2] E.J. Tobin, Recent coating developments for combination devices in orthopedic and dental applications: A literature review, Advanced Drug Delivery Reviews, 112 (2017) 88-100.
[3] Y. Li, C. Yang, H. Zhao, S. Qu, X. Li, Y. Li, New Developments of Ti-Based Alloys for Biomedical Applications, Materials, 7 (2014) 1709.
[4] L.T. Kuhn, Chapter 5 - Biomaterials A2 - Enderle, John D, in: J.D. Bronzino (Ed.) Introduction to Biomedical Engineering (Third Edition), Academic Press, Boston, 2012, pp. 219-271.
[5] X.P. Tan, Y.J. Tan, C.S.L. Chow, S.B. Tor, W.Y. Yeong, Metallic powder-bed based 3D printing of cellular scaffolds for orthopaedic implants: A state-of-the-art review on manufacturing, topological design, mechanical properties and biocompatibility, Materials Science and Engineering: C, 76 (2017) 1328-1343.
[6] S.H. Chen, S.C. Ho, C.H. Chang, C.C. Chen, W.C. Say, Influence of roughness on in-vivo properties of titanium implant surface and their electrochemical behavior, Surf. Coat. Technol., 302 (2016) 215-226.
[7] M. Khodaei, A. Valanezhad, I. Watanabe, R. Yousefi, Surface and mechanical properties of modified porous titanium scaffold, Surf. Coat. Technol., 315 (2017) 61-66.
[8] S.V. Dorozhkin, Calcium orthophosphate coatings, films and layers, Progress in Biomaterials, 1 (2012) 1.
[9] C.J. Li, W.Y. Li, Deposition characteristics of titanium coating in cold spraying, Surf. Coat. Technol., 167 (2003) 278-283.
[10] X. Nie, A. Leyland, A. Matthews, Deposition of layered bioceramic hydroxyapatite/TiO2 coatings on titanium alloys using a hybrid technique of micro-arc oxidation and electrophoresis, Surf. Coat. Technol., 125 (2000) 407-414.
[11] V.F. Pichugin, R.A. Surmenev, E.V. Shesterikov, M.A. Ryabtseva, E.V. Eshenko, S.I. Tverdokhlebov, O. Prymak, M. Epple, The preparation of calcium phosphate coatings on titanium and nickel-titanium by rf-magnetron-sputtered deposition: Composition, structure and micromechanical properties, Surf. Coat. Technol., 202 (2008) 3913-3920.
[12] A.A. Abdeltawab, M.A. Shoeib, S.G. Mohamed, Electrophoretic deposition of hydroxyapatite coatings on titanium from dimethylformamide suspensions, Surf. Coat. Technol., 206 (2011) 43-50.
[13] G.D. Byrne, L. O'Neill, B. Twomey, D.P. Dowling, Comparison between shot peening and abrasive blasting processes as deposition methods for hydroxyapatite coatings onto a titanium alloy, Surf. Coat. Technol., 216 (2013) 224-231.
[14] W. Xu, W. Hu, M. Li, C.e. Wen, Sol–gel derived hydroxyapatite/titania biocoatings on titanium substrate, Materials Letters, 60 (2006) 1575-1578.
[15] A.A.E. hadad, V. Barranco, A. Jiménez-Morales, E. Peon, J.C. Galván, Multifunctional sol-gel derived thin film based on nanocrystaline hydroxyapatite powders, Journal of Physics: Conference Series, 252 (2010) 012007.
[16] P. Usinskas, Z. Stankeviciute, A. Beganskiene and A. Kareiva. Sol-gel derived porous and hydrophilic calcium hydroxyapatite coating on modified titanium substrate. Surf. Coat. Technol., 307 (2016) 935-940

ACCEPTED MANUSCRIPT

[17] Y. Torres, J.J. Pavon, J.A. Rodriguez, Processing and characterization of porous titanium for implants by using NaCl as space holder, J. Mater. Process. Technol., 212 (2012) 1061-1069.
[18] W.J. Niu, C.G. Bai, G.B. Qiu, Q. Wang, Processing and properties of porous titanium using space holder technique, Mater. Sci. Eng. A-Struct. Mater. Prop. Microstruct. Process., 506 (2009) 148-151.
[19] Y. Torres, J.A. Rodríguez, S. Arias, M. Echeverry, S. Robledo, V. Amigo, J.J. Pavón, Processing, characterization and biological testing of porous titanium obtained by space-holder technique, Journal of Materials Science, 47 (2012) 6565-6576.
[20] D.-M. Liu, Q. Yang, T. Troczynski, W.J. Tseng, Structural evolution of sol–gel-derived hydroxyapatite, Biomaterials, 23 (2002) 1679-1687.
[21] A. El-Hadad, E. Peón, F.R. García-Galván, V. Barranco, J. Parra, A. Jiménez-Morales, J.C. Galván, Biocompatibility and Corrosion Protection Behaviour of Hydroxyapatite Sol-Gel Derived Coatings on Ti6Al4V Alloy Materials 2017, 10(2), 94, doi:10.3390/ma10020094. OPEN ACCESS.
[22] E. Peón, A. El-Hadad, F.R. García-Galván, A. Jiménez-Morales, J.C. Galván Controlled Rate Thermal Analysis (CRTA) as new method to control the specific surface of hydroxyapatite thin coatings. In "Modern Technologies for Creating the Thin-film Systems and Coatings". Book edited by Nikolay N. Nikitenkov. Publisher: InTech Open Access Publisher, Año de Publicación: 2017 Pág. inicial: 193 Pág. final:212, ISBN 978-953-51-3004-8, Print ISBN 978-953-51-3003-1, DOI: 10.5772/66468. OPEN ACCESS.
[23] A. A. El hadad, V. Barranco, A. Jiménez-Morales, E. Peón, G.J. Hickman, C.C. Perry, J.C. Galván, Enhancing in vitro biocompatibility and corrosion protection of organic-inorganic hybrid sol-gel films with nanocrystalline hydroxyapatite, Journal of Materials Chemistry B, 2, 3886-3896 (2014). DOI: 10.1039/C4TB00173G. OPEN ACCESS.
[24] Y. Torres, J.J. Pavon, I. Nieto, J.A. Rodriguez, Conventional powder metallurgy process and characterization of porous titanium for biomedical applications, Metall. Mater. Trans. B Process Metall. Mater. Process. Sci. 42 (4) (2011) 891–900.
[25] J. Banhart, Advanced tomographic methods in materials research and engineering, First ed., Oxford University Press, New York, 2008.
[26] ASM-International. Nondestructive evaluation and quality control. 9th ed. 1989.
[27] J. Müller-Rochholz, Determination of the elastic properties of lightweight aggregate by ultrasonic pulse velocity measurement, Int. J. Cem. Compos. Light. Concr. 1 (2) (1979) 87–90.
[28] ISO 13314. Mechanical testing of metals Ductility testing Compression test for porous and cellular metals (2011)
[29] W.E. Luecke, L. Ma, S.M. Graham, M.A. Adler, Repeatability and Reproducibility of Compression Strength Measurements Conducted According to ASTM E9, NIST Technical Note 1679, 2009.
[30] K. Mader, R. Mokso, C. Raufaste, B. Dollet, S. Santucci, J. Lambert, M. Stampanoni, Quantitative 3D characterization of cellular materials: Segmentation and morphology of foam, Colloids and Surfaces A: Physicochem. Eng. Aspects 415 (2012) 230– 238
[31] Y. Torres, C. Romero, Q. Chen, G. Pérez, Rodríguez-Ortiz JA, J. Pavón, L. Álvarez, C. Arévalo, A. Boccaccini, Electrophoretic Deposition of PEEK/45S5 Bioactive Glass Coating on Porous Titanium Substrate: Influence of Processing Conditions and Porosity Parameters, Key Engineering Materials, 704 (2016) 343-350.

ACCEPTED MANUSCRIPT

[32] S. Muñoz, J. Pavón, J.A. Rodríguez-Ortiz, A. Civantos, J.P. Allain, Y. Torres, On the influence of space holder in the development of porous titanium implants: Mechanical, computational and biological evaluation, Materials Characterization, 108 (2015) 68-78.
[33] X.-Z. Yin, T.-Q. Xiao, A. Nangia, S. Yang, X.-L. Lu, H.-Y. Li, Q. Shao, Y. He, P. York, J.-W. Zhang, In situ 3D topographic and shape analysis by synchrotron radiation X-ray microtomography for crystal form identification in polymorphic mixtures, Sci. Rep. 6, (2016) 24763.
[34] E. Maire, P. J. Withers, Quantitative X-ray tomography, International Materials Reviews 2014 VOL 59 No 1
[35] J. Tao, H. Pan, Y. Zeng, X. Xu, R. Tang, Roles of Amorphous Calcium Phosphate and Biological Additives in the Assembly of Hydroxyapatite Nanoparticles, J. Phys. Chem. B 2007, 111, 13410-13418
[36] E.P. Avés, G.F. Estévez, M.S. Sader, J.C.G. Sierra, J.C.L. Yurell, I.N. Bastos, G.D.A. Soares, Hydroxyapatite coating by sol–gel on Ti–6Al–4V alloy as drug carrier, Journal of Materials Science: Materials in Medicine, 20 (2009) 543-547.
[37] M.H. Fathi, A. Hanifi, Evaluation and characterization of nanostructure hydroxyapatite powder prepared by simple sol–gel method, Materials Letters, 61 (2007) 3978-3983.

ACCEPTED MANUSCRIPT

ACCEPTED MANUSCRIPT

FIGURE CAPTIONS

Figure 1. a) Optical microscopy image of the porous substrate. The 100-200 μm exposed value corresponds to the size range of the NH_4HCO_3 (ammonium hydrogen carbonate) spacer used; b) Confocal image; c) SEM micrographs of the porous titanium substrate; d) pore surface micro-roughness.

Figure 2. a) Microtomography 3D reconstruction image and distribution of porous roughness of titanium substrates for 100-200 μm NH_4HCO_3 particle size. Different colors show the segmented and separated pores. The Ti matrix is transparent. b) Distribution of roughness volume percentage in function of the porosity size, quantified as equivalent porosity diameter. An individual porous Ti disc substrate obtained by tomography is shown in the inset.

Figure 3. SEM micrographs of the obtained coating. Surface (a) and cross-sectional (b) views for 100-200 μm NH_4HCO_3 particle size used.

Figure 4. a) FTIR spectrum and b) XRD pattern of HA coating on porous titanium substrates for 100-200 μm NH_4HCO_3 particle size.

Figure 5. Confocal images for uncoated (a) and coated (b) titanium substrates.

Figure 6. Scratch test with increasing load in HA coating on porous titanium substrates for 100-200 μm NH_4HCO_3 particle size.

ACCEPTED MANUSCRIPT

ACCEPTED MANUSCRIPT

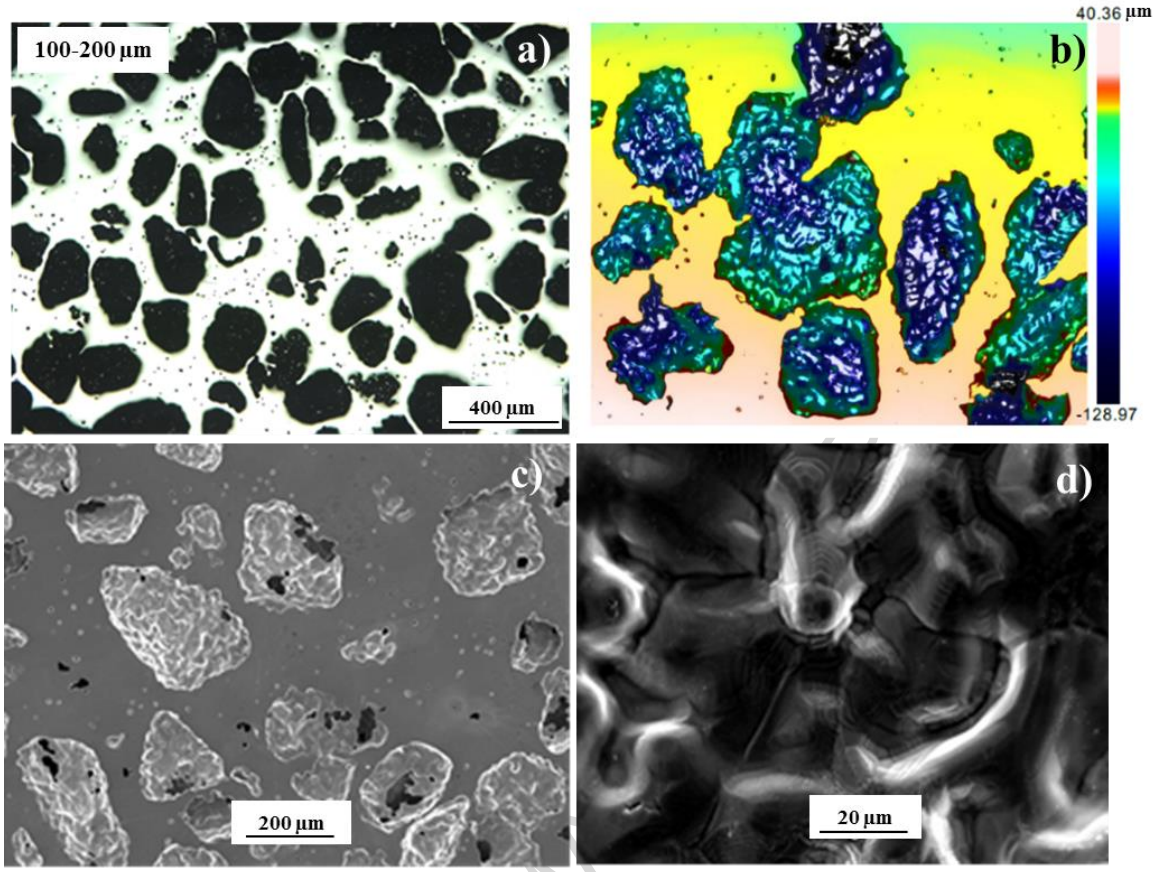

Figure 1

ACCEPTED MANUSCRIPT

ACCEPTED MANUSCRIPT

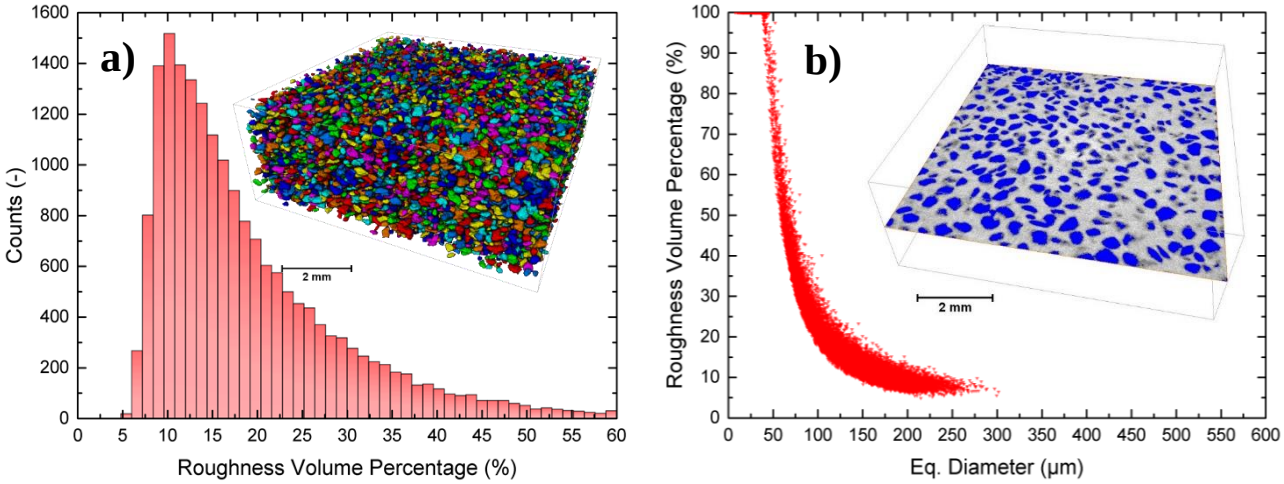

Figure 2

ACCEPTED MANUSCRIPT

ACCEPTED MANUSCRIPT

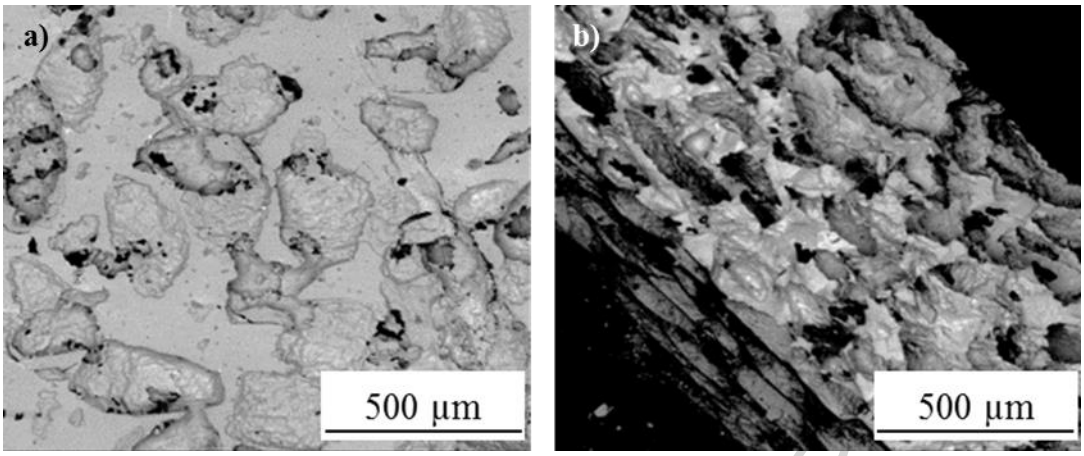

Figure 3

ACCEPTED MANUSCRIPT

ACCEPTED MANUSCRIPT

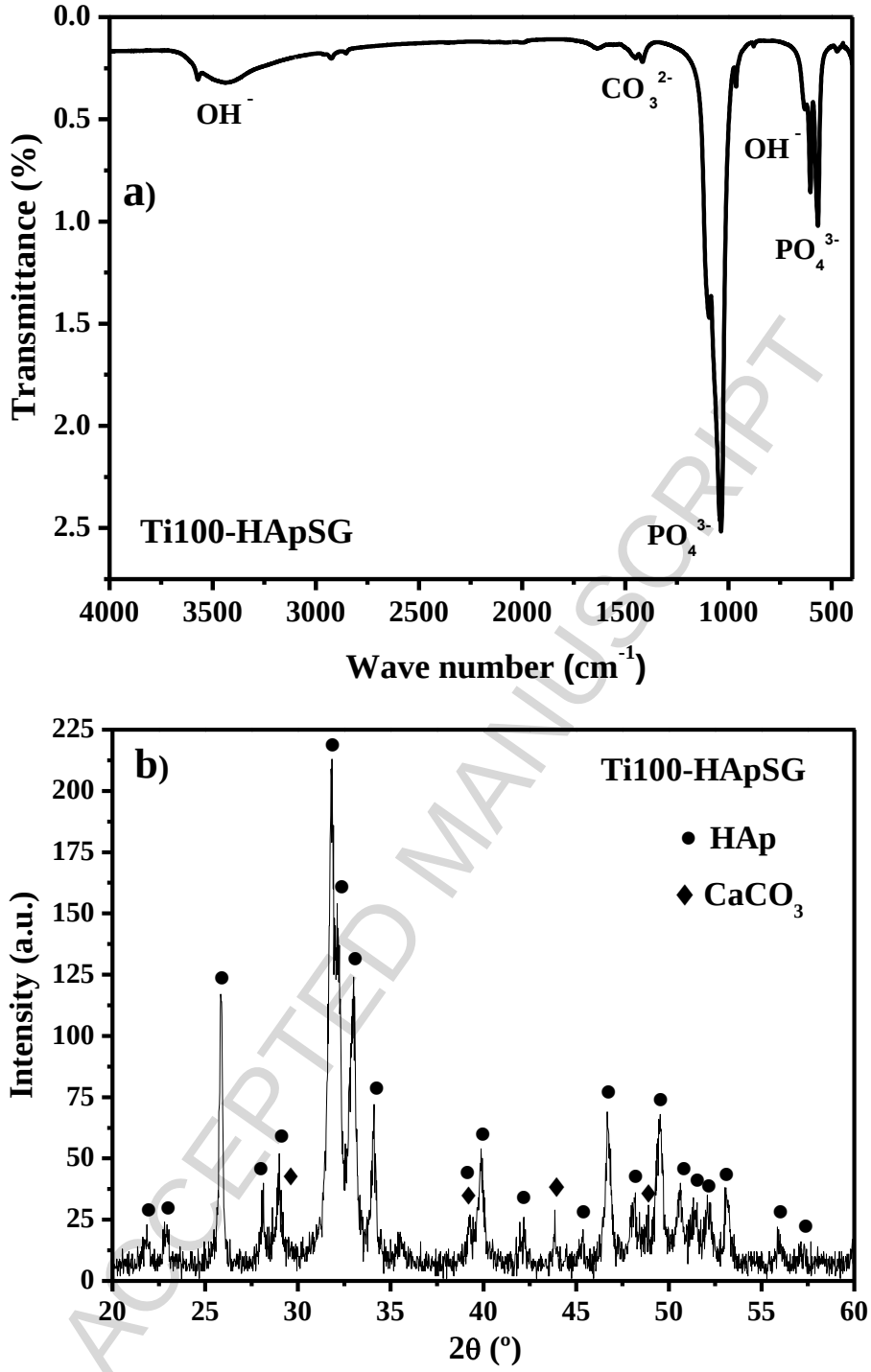

Figure 4

ACCEPTED MANUSCRIPT

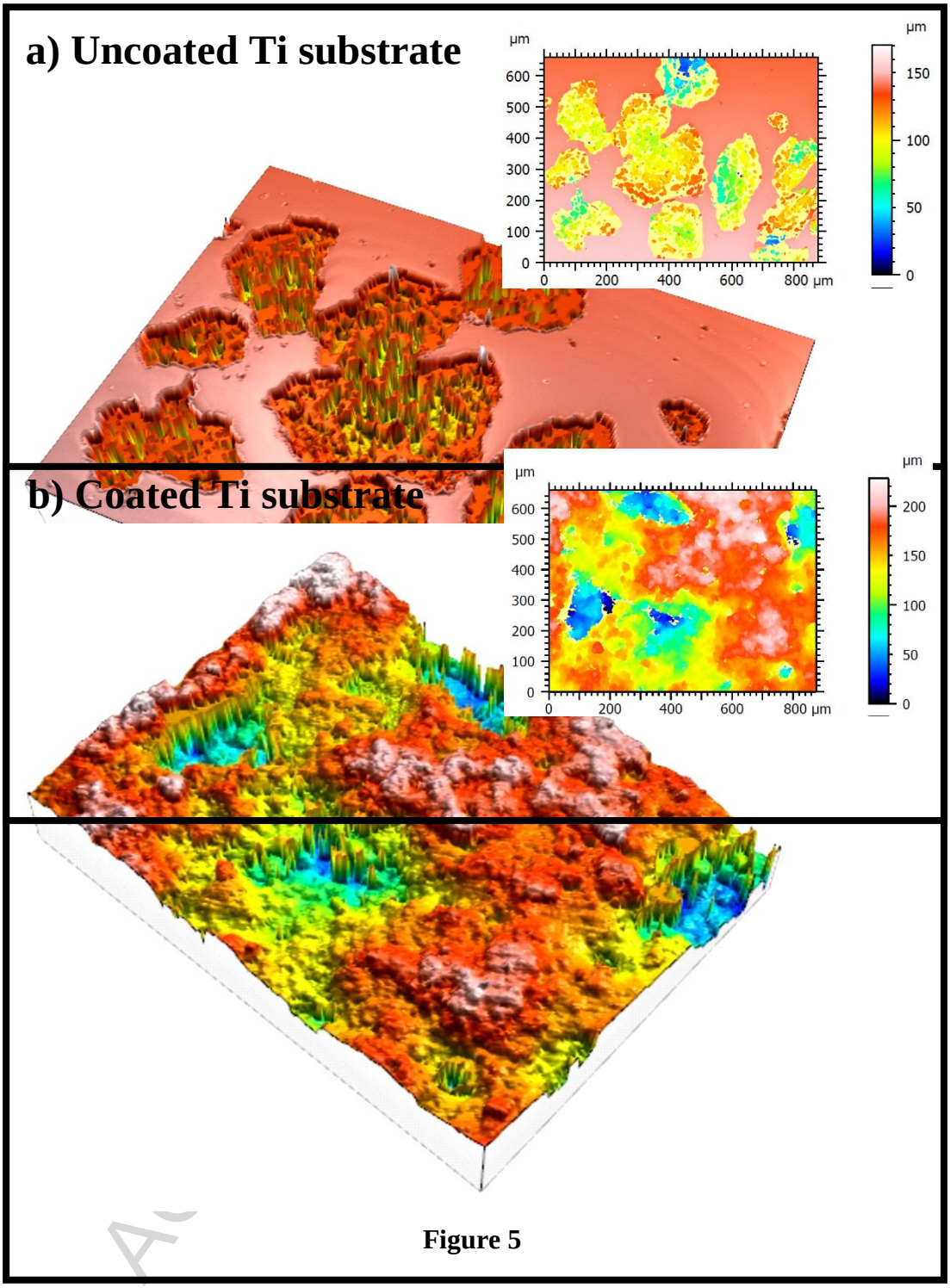

Figure 5

ACCEPTED MANUSCRIPT

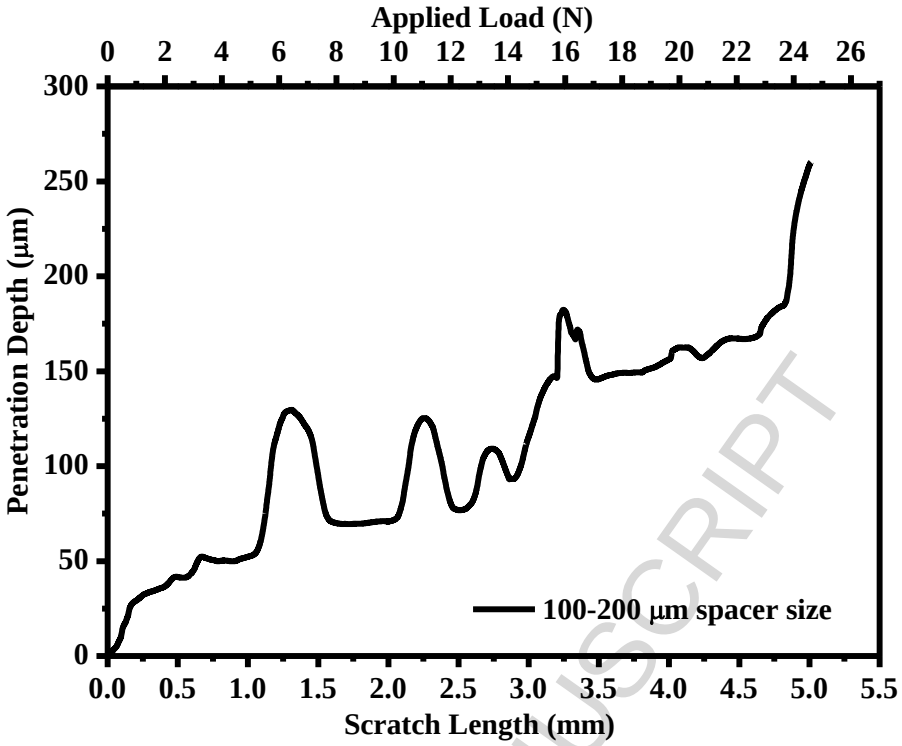

Figure 6

ACCEPTED MANUSCRIPT

ACCEPTED MANUSCRIPT

Highlights

- Porous Ti substrates were coated with hydroxyapatite by the sol-gel technique.
- A HA porous thin films onto the porous titanium substrates was obtained.
- The HA - porous Ti showed good mechanical interlocking and chemical bonding.
- The HA coatings can prevent the corrosion of Ti substrate and make it bioactive.
- The proposed HA coating on porous Ti allows a biofunctional and mechanical balance.

ACCEPTED MANUSCRIPT

View publication stats